Original Article
BR101801 enhances the radiosensitivity of p53-deficient colorectal cancer cells by inducing G2/M arrest, apoptosis, and senescence in a p53-independent manner

Mijeong Park[1], Jimin Ha[2], Yuri Lee[1,2], Youngjoo Kwon[1], Sang Hyun Choi[3], Byoung Soo Kim[4], Youn Kyoung Jeong[2]

[1]Graduate School of Pharmaceutical Sciences, College of Pharmacy, Ewha Womans University, Seoul 03760, Republic of Korea; [2]Radiological and Medical Support Center, Korea Institute of Radiological and Medical Sciences, Seoul 01812, Republic of Korea; [3]Research Team of Medical Physics and Engineering, Korea Institute of Radiological and Medical Sciences, Seoul 01812, Republic of Korea; [4]Division of Applied RI, Korea Institute of Radiological and Medical Sciences, Seoul 01812, Republic of Korea

Abstract: Inhibition of DNA-dependent protein kinase (DNA-PK) in the non-homologous end-joining repair pathway reportedly increases the radiation sensitivity of cancer cells. We have recently reported that BR101801, a novel triple inhibitor of PI3K-gamma (γ), delta (δ), and DNA-PK, functions as an efficient sensitizer of radiation-induced DNA damage in various human solid cancer cells and a xenograft mouse model. Given that the p53 tumor suppressor gene plays an important role in radiotherapeutic efficacy, in the current study, we focused on the impact of the p53 status on BR101801-induced radiosensitization using isogenic HCT116 p53$^{+/+}$ and HCT116 p53$^{-/-}$ human colorectal cancer cell lines. *In vitro*, HCT116 p53$^{+/+}$ and HCT116 p53$^{-/-}$ human colorectal cancer cells were pretreated with 1 µM BR101801 for 24 h before exposure to ionizing radiation (IR), followed by assays to analyze colony formation, DNA damage, cell cycle changes, senescence, autophagy, apoptosis, and DNA damage response-related proteins. Xenograft mouse models were constructed to examine the potential synergistic effects of BR101801 (50 mg/kg, orally administered once daily) and fractionated IR (2 Gy × 3 days) on tumor growth inhibition *in vivo*. BR101801 inhibited cell proliferation and prolonged DNA damage in both HCT116 p53$^{+/+}$ and HCT116 p53$^{-/-}$ human colorectal cancer cells. Combined treatment with BR101801 and IR robustly induced G2/M phase cell cycle arrest, apoptosis, and cellular senescence in HCT116 p53$^{-/-}$ cells when compared with treatment with IR alone. Furthermore, BR101801 synergistically inhibited tumor growth in the HCT116 p53$^{-/-}$ xenograft mouse model. BR101801 enhanced the radiosensitivity of HCT116 human colorectal cancer cells regardless of their p53 status. Moreover, BR101801 exerted robust synergistic effects on IR-induced cell cycle arrest, apoptosis, and tumor growth inhibition, even in radioresistant HCT116 p53$^{-/-}$ cells. Overall, these findings provide a scientific rationale for combining BR101801 with IR as a new therapeutic strategy to overcome radioresistance induced by p53 deficiency.

Keywords: Radioresistance, DNA-PK inhibitor, radiosensitizer, p53-deficiency, colorectal cancer cells, xenograft mouse model

Introduction

Colorectal cancer (CRC) is the third most common malignant tumor globally, with a high mortality rate. In 2020 alone, approximately 1.9 million CRC cases were reported worldwide, with the number estimated to increase to 3.2 million by 2040 [1]. Given the rising incidence of CRC in individuals under the age of 50, the American Cancer Society recommends initiating CRC screening at age 45 to ensure timely disease detection [2]. Radiation therapy is conventionally employed before and after surgery for stage 2 or 3 advanced CRC, well-characterized by a high risk of recurrence [3].

The p53 gene, a tumor suppressor, exhibits low expression levels under normal circumstances.

However, its expression is found to be elevated in response to radiation-induced DNA damage. As a DNA damage response (DDR), p53 is involved in cell cycle arrest, apoptosis, and cellular senescence and plays an important role in determining cell fate depending on the degree of cell damage [4]. However, p53 is reportedly mutated in 4-50% of patients with CRC, which is one of the important factors contributing to increased resistance to radiation therapy [5]. Resistance to radiation therapy eventually fails to suppress the aggressive and metastatic nature of CRC, resulting in poor treatment prognosis. Therefore, to overcome radiation resistance induced by p53 mutations or deficiencies in CRC, developing an effective treatment strategy could improve radiotherapy outcomes.

Radiosensitizers have demonstrated advantages in radiation therapy by amplifying DNA damage, a major biological consequence of radiation exposure. The augmented DNA damage is coupled with an indirect increase in cytotoxicity mediated by reactive oxygen species, thereby minimizing damage to normal tissues. The net effect is an increased efficacy of radiation therapy, effectively eliminating cancer cells [6]. Radiation-induced DNA double-strand breaks (DSB) are repaired via homologous recombination (HR) and non-homologous end-joining (NHEJ) pathways [7, 8]. Accordingly, inhibitors targeting several factors involved in the DSB repair pathway can function as radiosensitizers by prolonging the persistence of radiation-induced DSB. DNA-dependent protein kinase (DNA-PK) is one of the main factors involved in DSB repair via NHEJ [9, 10]. Accumulated evidence suggests that DNA-PK inhibitors, such as NU7441, M3814, AZD7648, and BR101801, can enhance ionizing radiation (IR)-induced antitumor effects, including cell cycle arrest, apoptosis, cellular senescence, and DNA repair inhibition [11-14]. In particular, both NU7441 and M3814 can overcome radioresistance by eliciting radiosensitivity even in the presence of p53 deficiency [11, 12].

In our previous study, for the first time, we reported the synergistic radiosensitizing effect of BR101801 as a novel triple inhibitor of PI3K-gamma (γ), delta (γ), and DNA-PK in several solid tumors [14]. Notably, the combined impact of BR101801 and IR exhibited greater efficacy in HT-29 CRC cells bearing a mutant p53 than in HCT116 CRC cells with wild-type p53.

Accordingly, BR101801 may play distinct roles depending on the p53 status in CRC cells, although the relationship between BR101801, p53 status, and antitumor efficacy remains elusive. Therefore, in the current study, we aimed to determine the impact of p53 status on BR101801-mediated radiosensitivity both *in vitro* and *in vivo* using paired isogenic HCT116 p53$^{+/+}$ and HCT116 p53$^{-/-}$ human CRC cells.

Materials and methods

Chemicals

BR101801 was provided by Boryung Pharmaceutical (Ansan, Gyeonggi-do, Republic of Korea). For *in vitro* experiments, BR101801 was dissolved in dimethyl sulfoxide (DMSO) to obtain a 10 mmol/L stock solution, stored at -20°C until use. Cells were treated with 1 μM BR101801 for 24 h before IR; the concentration was selected based on a synergistic radiosensitization effect observed in various human solid cancer cells in our previous study [14]. For *in vivo* experiments, a 50 mg/kg of BR101801 was prepared in a 200 μL mixture of 5% DMSO/55% PEG400/40% distilled water, followed by storage at 4°C for up to 1 week.

Antibody

Anti-cyclin B1 antibody (cat. no. 4138), anti-phospo-cdc2 (Tyr15) (cat. no. 9111), anti-CHK2 (cat. no. 2662), anti-phospo-CHK2 (Thr68) (cat. no. 2661), anti-PARP (cat. no. 9542), anti-p53 (cat. no. 9282), and anti-LC3B I/II (cat. no. 2775) were obtained from Cell Signaling Technology (Danvers, MA, USA). Anti-Rad51 (cat. no. 53428), anti-p21 (cat. no. 397), and anti-GAPDH (cat. no. 25778) were purchased from Santa Cruz Biotechnology (Dallas, TX, USA).

Cell lines and culture

HCT116 p53$^{+/+}$ human CRC cell line was purchased from the Korean Cell Line Bank (KCLB No. 10247), and HCT116 p53$^{-/-}$ cell line was supplied by Dr. B. Vogelstein (Johns Hopkins University, Baltimore, MD, USA). Both HCT116 p53$^{+/+}$ and HCT116 p53$^{-/-}$ cells were cultured in RPMI 1640 media containing 10% (v/v) fetal bovine serum (FBS), 100 U/mL penicillin, and 100 μg/mL streptomycin, followed by incubation in a CO$_2$ incubator (5% CO$_2$ at 37°C).

Gamma-ray IR

Cells were seeded in a 60 mm cell culture dish and irradiated using a ^{137}Cs gamma-ray irradiator (Gammacell 3000 Elan; Atomic Energy of Canada Ltd., Ontario, Canada) at a rate of 2.24 Gy/min.

Colony formation assay

Briefly, cells were seeded in triplicate in 60 mm cell culture dishes, with varying cell counts of 300, 600, 1200, and 2400 cells at radiation doses of 0, 2, 4, and 6 Gy, respectively. Then, cells were pretreated with 1 µM BR101801 for 24 h before IR. Twenty-four hours after IR, media were replaced with a fresh culture medium, and cells were cultured for 7 days in the CO_2 incubator (5% CO_2 at 37°C). After formation, colonies were fixed with cold methanol and stained with crystal violet.

Immunocytochemistry

Briefly, cells were seeded onto coverslips in 24-well plates overnight and pretreated with 1 µM BR101801 for 24 h. After either 1 or 24 h of exposure to IR at a dose of 4 Gy, cells were fixed with 4% paraformaldehyde and incubated with 0.5% Triton X-100 for permeabilization. Then, cells were incubated with 4% bovine serum albumin for blocking and incubated with anti-γ-H2AX overnight at 4°C. For immunofluorescence, the cells were incubated with FITC-labeled goat anti-mouse IgG for 1 h and stained with DAPI (1 mg/mL) to visualize nuclei. The cells were washed with phosphate-buffered saline, mounted onto slides, and imaged using fluorescence microscopy (AxioImager.M2, Zeiss, Jena, Germany).

Cell cycle

Cells were seeded in a 60 mm cell culture dish overnight and irradiated at 4 Gy after 24 h of pretreatment with 1 µM BR101801. After 24 h or 48 h of IR, cells were harvested and fixed with 70% cold ethanol. Next, cells were stained with BD PI/RNase staining buffer (BD Biosciences, San Diego, CA, USA). The cell cycle was analyzed using a CytoFLEX Flow Cytometer (Beckman Coulter, Brea, CA, USA).

Autophagy analysis

Briefly, cells were seeded onto coverslips in 24 well plates overnight and irradiated (4 Gy) 24 h after pretreatment with 1 µM BR101801. Twenty-four hours after IR, cells were stained for autophagy detection using a CYTO-ID Autophagy Detection Kit (cat. ENZ-51031; Enzo Life Sciences, Farmingdale, NY, USA) according to the manufacturer's protocol and photographed using a fluorescence microscope (AxioImager.M2, Zeiss, Jena, Germany).

Cellular senescence

Briefly, cells were seeded in 6 well plates overnight and irradiated (4 Gy) 24 h after pretreatment with 1 µM BR101801. Twenty-four hours after IR, cellular senescence was assessed using a senescence-galactosidase staining kit (cat. 9860; Cell Signaling Technology, Beverly, MA, USA) following the manufacturer's protocol and photographed using a light microscope (Motic AE31 microscope, Ted Pella Inc., Redding, CA, USA).

Apoptosis analysis

Briefly, cells were seeded in a 60 mm cell culture dish overnight and irradiated (4 Gy) 24 h after pretreatment with 1 µM BR101801. Seventy-two hours after IR, cells were stained using an Annexin V-FITC Apoptosis Detection Kit according to the manufacturer's protocol (cat. 556570; BD Biosciences, San Diego, CA, USA) and analyzed using a CytoFLEX Flow Cytometer (Beckman Coulter, Brea, CA, USA).

Western blotting analysis

Cellular proteins were extracted using a mixture of RIPA cell lysis buffer, phosphates, and a protease inhibitor cocktail (GenDEPOT, Katy, TX, USA). Total protein concentrations were measured following the Bradford protein assay using the Bio-Rad protein assay reagent (Bio-Rad Laboratories, Hercules, CA, USA). Proteins (20 µg) were separated by sodium dodecyl sulfate-polyacrylamide gel electrophoresis (PAGE) and transferred to poly (polyvinylidene fluoride) membranes. Subsequently, membranes were blocked with blocking buffer (cat. 12010020; Bio-Rad Laboratories, Hercules, CA, USA) for 10 min and incubated with primary antibodies overnight at 4°C. The membranes were washed with TBST and incubated with horseradish peroxidase-conjugated secondary antibodies for 1 h at room temperature. Protein bands were detected using an enhanced chemiluminescence (ECL) immunoblotting substrate (Bio-Rad Laboratories, Hercules, CA, USA) and

ImageQuant LAS 4000 mini (GE Healthcare, Chicago, IL, USA).

Xenograft mouse model

Four-week-old Blab/c nude male mice were obtained from Orient Bio Inc. (Gapyeong, Korea) and maintained in an individually ventilated cage system with a 12 h light/dark cycle (lights on at 8:00 AM). HCT116 p53$^{+/+}$ and HCT116 p53$^{-/-}$ cells (3×10^6 cells/100 µL) were subcutaneously injected into the right thigh of mice. The tumor volume was measured using a caliper according to the following formula: tumor volume (mm^3) = ([smaller diameter]^2 × [larger diameter] × π/6). When the tumor volume reached approximately 200 mm^3, mice were orally administered vehicle (5% DMSO, 55% PEG400, 40% distilled water) or BR101-801 (50 mg/kg/day). After two days of treatment, tumors in the mouse legs were locally irradiated with 2 Gy for 3 days using a ^{60}Co gamma-ray irradiator (GammaBeam™ 100-80, Best Theratronics Ltd., Kanata, ON, Canada) at a dose rate of 0.85 Gy/min. When the tumor volume of the vehicle group reached approximately 1000 mm^3, mice were euthanized using CO_2, and tumors were excised and weighed. All animal experiments were conducted in accordance with the guidelines of the Institutional Animal Care and Use Committee of the Korea Institute of Radiological and Medical Sciences (IACUC No. KIRAMS 2022-0089).

Statistical analysis

All graphs were generated using GraphPad Prism 9.5 (La Jolla, CA, USA). Data are presented as the mean ± standard error of the mean (SEM). Statistical analysis was performed by student's *t*-test to compare the mean value between two groups using SPSS Statistics 23.0 (IBM Corp., Armonk, NY, USA) and statistical significant was considered at $^*P < 0.05$, $^{**}P < 0.01$, and $^{***}P < 0.001$.

Results

BR101801 enhanced the radiosensitivity of HCT116 p53$^{+/+}$ and HCT116 p53$^{-/-}$ cells

Clonogenic cell survival was analyzed to assess the radiosensitizing effect of BR101801 in HCT116 p53$^{+/+}$ and HCT116 p53$^{-/-}$ cells. Cells were pretreated with 1 µM BR101801 for 24 h, followed by irradiation with 2, 4, or 6 Gy of radiation. In both HCT116 p53$^{+/+}$ and HCT116 p53$^{-/-}$ cells, there were no differences in the survival fraction following treatment with 1 µM BR101801 at 0 Gy. Combined treatment with BR101801 and IR significantly reduced clonogenic survival fraction when compared with IR alone in HCT116 p53$^{+/+}$ cells (2 Gy: IR = 0.288, BR101801 + IR = 0.080, $P < 0.001$; 4 Gy: IR = 0.019, BR101801 + IR = 0.008, $P < 0.01$) (**Figure 1A**). In addition, combined treatment with BR101801 and IR significantly reduced the clonogenic survival fraction in HCT116 p53$^{-/-}$ cells (2 Gy: IR = 0.615, BR101801 + IR = 0.218, $P < 0.01$; 4 Gy: IR = 0.052, BR101801 + IR = 0.020, $P < 0.05$) (**Figure 1B**). Overall, these results suggest that BR101801 could induce a radiosensitizing effect in both the radiosensitive HCT116 p53$^{+/+}$ cells and radioresistant HCT116 p53$^{-/-}$ cells.

BR101801 impaired IR-induced DSB repair and altered protein expression related to IR-induced DDR in both HCT116 p53$^{+/+}$ and HCT116 p53$^{-/-}$ cells

To determine the mechanism through which p53 status affects IR-induced DDR in the presence of BR101801, we performed immunostaining for γ-H2AX, a DNA damage marker, in both HCT116 p53$^{+/+}$ and HCT116 p53$^{-/-}$ cells (**Figure 2**). The IR alone group exhibited increased γ-H2AX expression 1 h after IR, which subsequently decreased 24 h after IR in both HCT116 p53$^{+/+}$ and p53$^{-/-}$ cells. However, combined treatment with BR101801 and IR prolonged the increased γ-H2AX expression in both HCT116 p53$^{+/+}$ and HCT116 p53$^{-/-}$ cells. To further explore the effects of BR101801 on IR-induced DNA damage based on p53 status, we analyzed cell morphology and several protein markers 24 h after IR in HCT116 p53$^{+/+}$ and HCT116 p53$^{-/-}$ cells. BR101801 induced morphological changes in both HCT116 p53$^{+/+}$ and HCT116 p53$^{-/-}$ cells, but a greater effect was observed in HCT116 p53$^{+/+}$ cells (**Figure 3A**). In HCT116 p53$^{+/+}$ cells, treatment with IR alone upregulated the expression of Rad51, cyclin B1, p-cdc2, and p53 activation when compared with control treatment; however, BR101801 combined with IR downregulated these expression patterns (**Figure 3B**). Likewise, treatment with IR alone upregulated the expression of Rad51, cyclin B1, p-cdc2, and
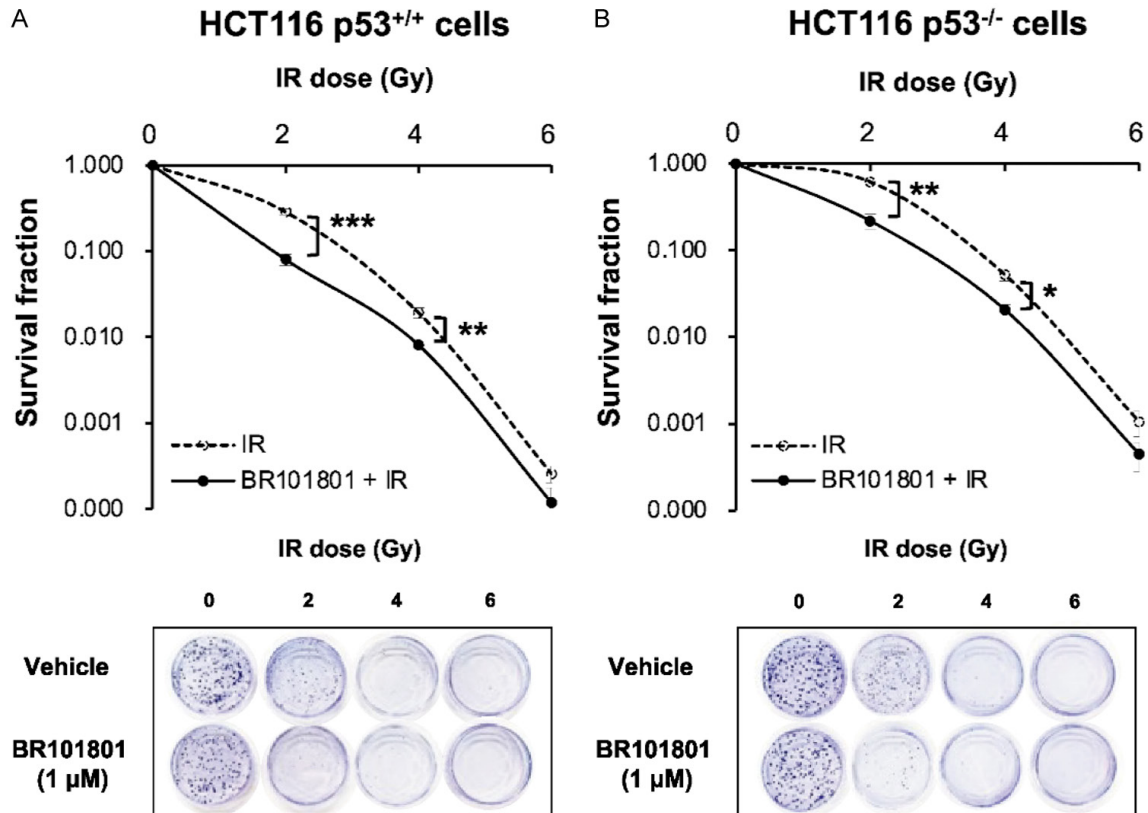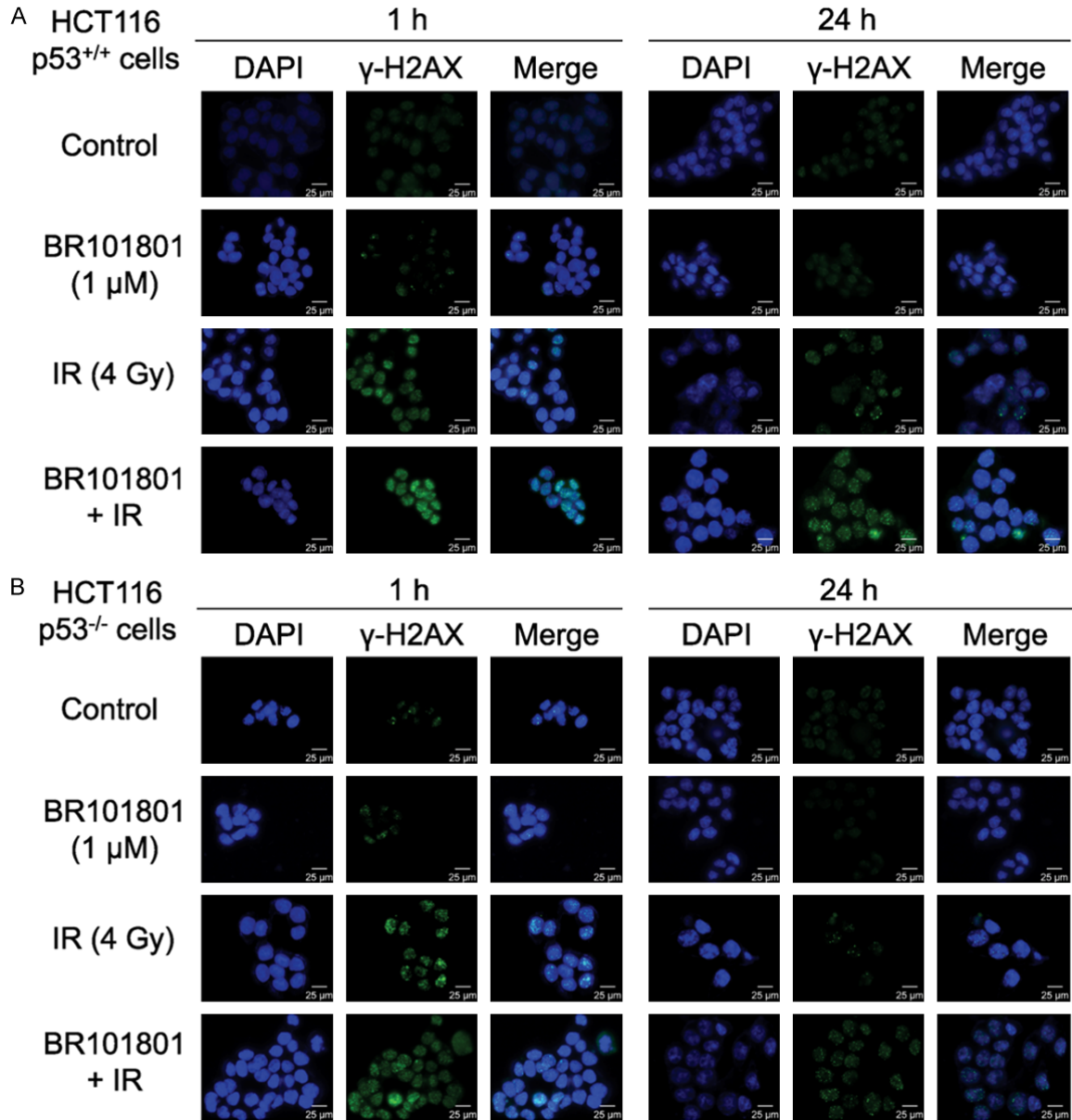
Figure 1. BR101801 synergistically increases radiosensitivity in human colorectal cancer cell lines. HCT116 p53$^{+/+}$ and HCT116 p53$^{-/-}$ cells were pretreated with 1 μM BR101801 for 24 h followed by irradiation with various doses of ^{137}Cs gamma-ray and allowed to grow for 7 days. Survival curves and representative colony formation images of (A) HCT116 p53$^{+/+}$ cells and (B) HCT116 p53$^{-/-}$ cells were obtained from the results of the colony formation assay. All data values are presented as the mean of four independent experiments ± standard error of the mean (SEM) (*$P < 0.05$, **$P < 0.01$, ***$P < 0.001$).

p21 activation in HCT116 p53$^{-/-}$ cells when compared with control treatment; however, BR101801 downregulated these patterns when compared with IR alone treatment. Notably, combination treatment with BR101801 and IR induced greater p-CHK2 upregulation than treatment with IR alone in HCT116 p53$^{-/-}$ cells (**Figure 3B**). These results suggest that combining BR101801 and IR delayed the repair of IR-induced DNA damage and altered protein expression related to the IR-induced DDR; these effects were independent of the p53 status of HCT116 cells.

Combination treatment with BR101801 and IR induced cell cycle arrest at subG1 and G2/M phases depending on p53 status

Cell cycle distribution was analyzed to determine the effects of BR101801 on IR-induced cell cycle accumulation according to the p53

status of HCT116 cells. In HCT116 p53$^{+/+}$ cells, treatment with IR alone induced cell cycle arrest at the G2/M phase when compared with control treatment (24 h: $P < 0.05$, 48 h: $P < 0.001$). Combining BR101801 and IR increased the proportion of G2/M phase when compared with control treatment after 48 h ($P < 0.01$) and also increased subG1 phase when compared with IR alone treatment (24 h: $P < 0.05$, 48 h: $P = 0.05$) (**Figure 4A**). In HCT116 p53$^{-/-}$ cells, treatment with IR alone increased the proportion of cells in the G2/M phase when compared with control treatment (24 h: $P < 0.001$, 48 h: $P < 0.05$); combined treatment with BR101801 and IR markedly increased G2/M phase cell cycle arrest when compared with IR alone treatment after 48 h ($P < 0.01$) (**Figure 4B**). Collectively, these results suggest that combined treatment with BR101801 and IR could induce cell cycle arrest during different phases depending on the p53 status.
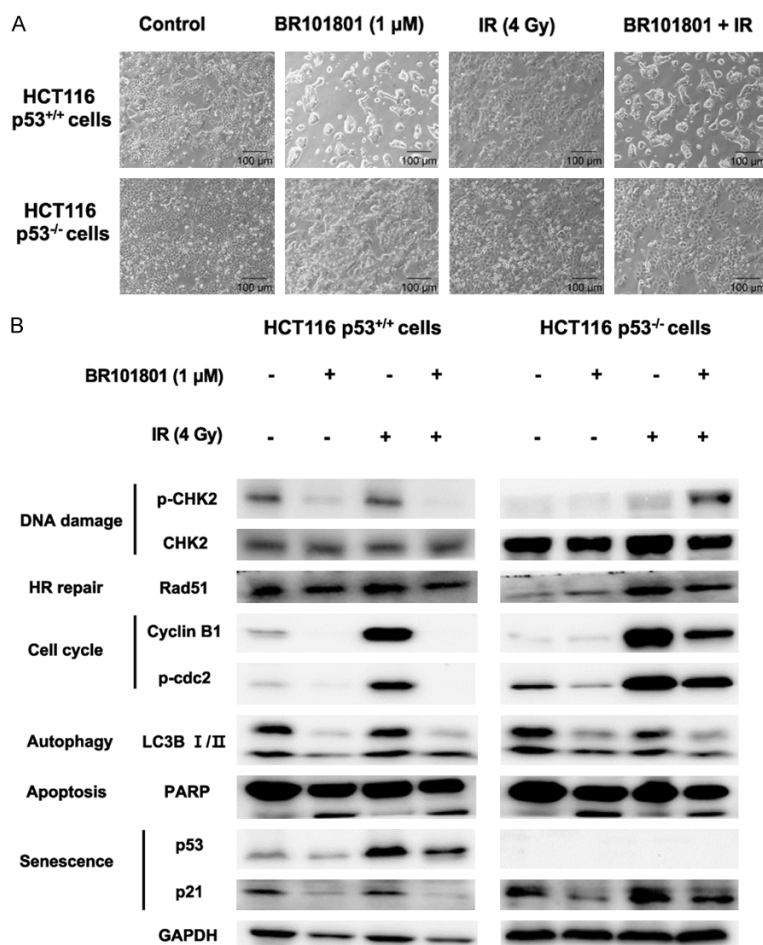
Figure 2. BR101801 prolongs IR-induced DNA damage in human colorectal cancer cell lines. HCT116 p53^{+/+} and HCT116 p53^{-/-} cells were pretreated with 1 μM BR101801 for 24 h and irradiated with 4 Gy. After 1 or 24 h of IR, cells were stained with DAPI (blue; nuclei marker) and anti-γ-H2AX (green; DNA damage marker). Representative images of (A) HCT116 p53^{+/+} cells and (B) HCT116 p53^{-/-} cells were acquired using a fluorescence microscope. Scale bar = 25 μm (magnification, 100 ×). IR, ionizing radiation.

BR101801 accelerated IR-induced autophagy in HCT116 p53^{+/+} cells and cellular senescence in HCT116 p53^{-/-} cells

To determine the effects of p53 status on the IR-induced autophagy mediated by BR101801, immunofluorescence analysis of autophagic vacuoles was performed by subjecting HCT116 p53^{+/+} and HCT116 p53^{-/-} cells to CYTO-ID staining (**Figure 5**). Combined treatment with BR101801 and IR increased the number of green-labeled vacuoles in HCT116 p53^{+/+} cells but not in HCT116 p53^{-/-} cells. To further examine the effects of p53 status on IR-induced cellular senescence mediated by BR101801, HCT116 p53^{+/+} and HCT116 p53^{-/-} cells were subjected to senescence-associated β-galactosidase (SA-β-gal) staining (**Figure 6**). In

Figure 3. BR101801 modulates the expression of IR-related mechanistic proteins in human colorectal cancer cell lines. HCT116 p53$^{+/+}$ and HCT116 p53$^{-/-}$ cells were pretreated with 1 μM BR101801 for 24 h and irradiated with 4 Gy. After 24 h of IR, cells were harvested, followed by protein extraction. A. Cell morphology of HCT116 p53$^{+/+}$ and HCT116 p53$^{-/-}$ cells. Representative images were acquired by performing light microscopy. Scale bar = 100 μm (magnification, 20 ×). B. The protein expression of DNA damage marker (CHK2 and p-CHK2), HR pathway of DNA repair marker (Rad51), G2/M checkpoint regulators (cyclin B1 and p-cdc2), autophagy marker (LC3B I/II), apoptosis marker (PARP), and senescence marker (p53 and p21) were measured by western blotting. HR, homologous recombination; IR, ionizing radiation.

edly accelerated IR-induced cellular senescence in HCT-116 p53$^{-/-}$ cells when compared with that in HCT116 p53$^{+/+}$ cells.

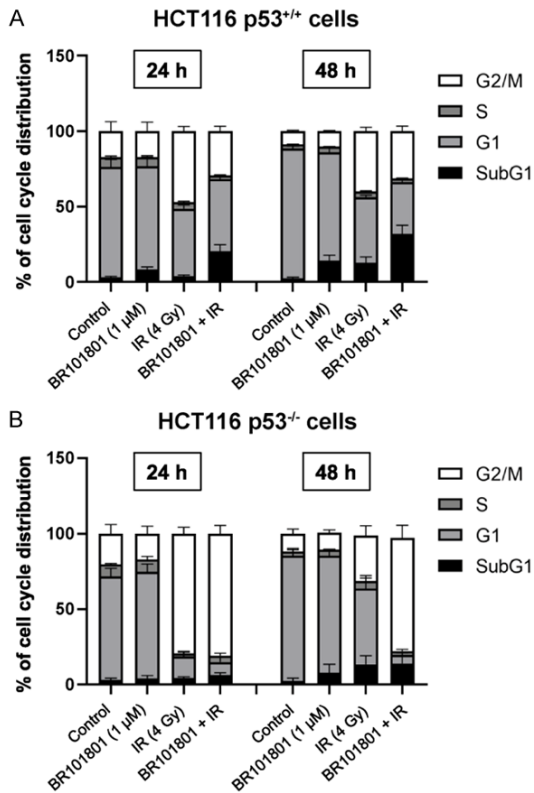*BR101801 exerted greater IR-induced apoptosis in HCT116 p53$^{-/-}$ cells than in HCT116 p53$^{+/+}$ cells*

To determine the impact of p53 status on cellular apoptosis mediated by BR101801 combined with IR, HCT116 p53$^{+/+}$ and HCT116 p53$^{-/-}$ cells were subjected to Annexin V staining followed by flow cytometry (**Figure 7A**). In HCT-116 p53$^{+/+}$ cells, combined treatment with BR101801 and IR significantly increased the proportion of apoptotic cells when compared with control treatment ($P < 0.05$); however, IR alone did not increase apoptosis ($P > 0.05$) when compared with control treatment (**Figure 7B**). In HCT116 p53$^{-/-}$ cells, IR alone also increased the proportion of apoptotic cells when compared with control treatment ($P < 0.01$), and combined treatment with BR101801 and IR robustly enhanced apoptosis when compared with that induced by the control ($P < 0.001$) and IR alone ($P < 0.01$) treatments (**Figure 7C**). These results suggest that combining BR101801 and IR could significantly increase cellular apoptosis, and IR-induced apoptosis was markedly enhanced in p53-deficient cells when compared with that in p53 wild-type cells.

BR101801 exerted antitumor efficacy in the HCT116 p53$^{-/-}$ xenograft mouse model

To determine the impact of p53 status on the antitumor efficacy of BR101801, we generated xenograft mouse models using paired isogenic human CRC cell lines, HCT116 p53$^{+/+}$ and

HCT116 p53$^{+/+}$ cells, SA-β-gal activity was detected in cells treated with BR101801, IR, and BR101801 combined with IR. In HCT116 p53$^{-/-}$ cells, treatment with IR alone and combined treatment with BR101801 and IR induced SA-β-gal activity, whereas BR101801 alone did not induce this activity. Taken together, these results suggest that BR101801 could accelerate IR-induced autophagosome formation in HCT116 p53$^{+/+}$ cells and IR-induced cellular senescence in both HCT116 p53$^{+/+}$ and HCT116 p53$^{-/-}$ cells; however, BR101801 mark-

Figure 4. BR101801 blocks cell cycle progression by inducing arrest at subG1 and G2/M phase in human colorectal cancer cell lines. HCT116 p53^{+/+} and HCT116 p53^{-/-} cells were pretreated with 1 µM BR101801 for 24 h and irradiated with 4 Gy. After 24 or 48 h of IR, the percentage of cells in subG1, G1, S, and G2/M phases of the cell cycle was analyzed using flow cytometry. Combined treatment with BR101801 and IR increases the percentage of the subG1 phase (A) in the HCT116 p53^{+/+} cells and the percentage of the G2/M phase (B) in the HCT116 p53^{-/-} cells. All data values are presented as the mean of three independent experiments ± standard error of the mean (SEM). IR, ionizing radiation.

HCT116 p53^{-/-} cells. When the tumor volume of the vehicle group reached ~1000 mm³, tumors of all groups were excised, and tumor weights were compared between groups. In the HCT116 p53^{+/+} xenograft mouse model, there were no notable differences in response to BR101801, IR or combination treatment with BR101801 and IR in terms of both tumor volume and weight when compared with the vehicle-treated group (**Figure 8A**, **8B**). Conversely, in the HCT116 p53^{-/-} xenograft mouse model, combined treatment with BR101801 and IR substantially reduced tumor growth at the experimental endpoint; this reduction was significantly pronounced when compared with that

induced by vehicle ($P < 0.001$), BR101801 ($P < 0.01$), and IR ($P < 0.05$) treatment (**Figure 8C**). Moreover, combined treatment with BR101801 and IR significantly reduced tumor weight when compared with the vehicle-treated ($P < 0.01$), BR101801-treated ($P < 0.001$), and IR-treated ($P < 0.05$) groups (**Figure 8D**). Overall, these results suggest that BR101801 has the potential to enhance antitumor efficacy in a p53-deficient, but not in a p53 wild-type, xenograft mouse model by improving radiosensitivity.

Discussion

BR101801, a novel drug candidate for lymphoma treatment, has been shown to simultaneously inhibit PI3K-γ/δ and DNA-PK, both known to play a crucial role in cancer cell growth and regulation [14, 15]. BR101801 is currently in phase 1 clinical trials for adult patients with advanced hematologic malignancies (ClinicalTrials.gov Identifier: NCT04018-248). In 2022, BR101801 was designated an orphan drug for treating of peripheral T-cell lymphoma by the US Food and Drug Administration. In a recent report, we revealed the role of BR101801 as a radiosensitizer in various solid tumors, as demonstrated by an enhanced radiation response, accumulation of G2/M phase cells, delayed DNA repair, and substantial reduction in DNA-PK protein levels [14]. Given that p53, a tumor suppressor gene, plays an important role in radiation-induced DDR and affects radiotherapeutic efficacy [16-18], it is crucial to comprehensively clarify the relationship between BR101801 as a radiosensitizer and p53 status in cancer. To the best of our knowledge, the current study is the first to determine the effects of p53 status on the radiosensitivity of BR101801 using paired isogenic HCT116 p53^{+/+} and HCT116 p53^{-/-} human CRC cells *in vitro* and *in vivo*. The present study provides a scientific rationale for combining BR101801 and IR as a new therapeutic strategy to overcome radioresistance induced by p53 deficiency.

It is well-documented that cancer cells with wild-type p53 reportedly exhibit greater radiosensitivity than those with p53 mutations or deficiency [19-21]. In the present study, by comparing survival fraction at 2 Gy (SF2) as a marker of radiation dose-response, we found that HCT116 p53^{+/+} cells with an SF2 of 0.288
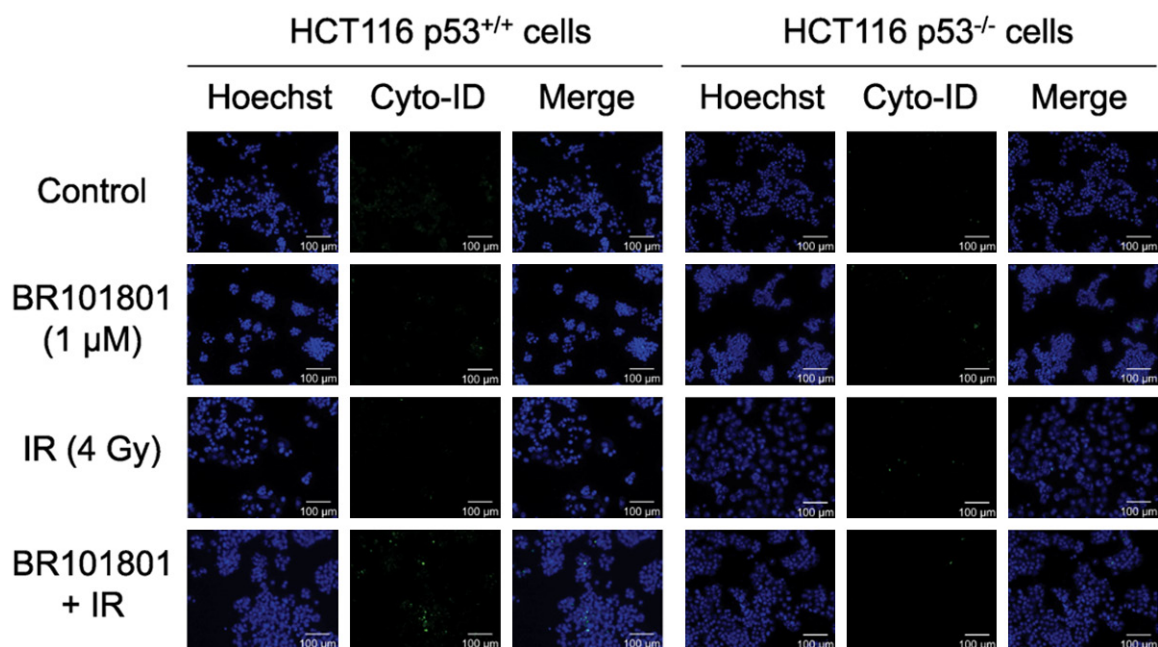
Figure 5. Combined treatment with BR101801 and IR increases autophagic vacuoles in HCT116 p53$^{+/+}$ cells. HCT116 p53$^{+/+}$ and HCT116 p53$^{-/-}$ cells were pretreated with 1 μM BR101801 for 24 h and irradiated with 4 Gy. After 24 h of IR, cells were stained with Cyto-ID dye (green; autophagosome marker) and Hoechst 33342 dye (blue; nuclear staining). Representative images were acquired using a fluorescence microscope. Scale bar = 100 μm (magnification, 20 ×). IR, ionizing radiation.
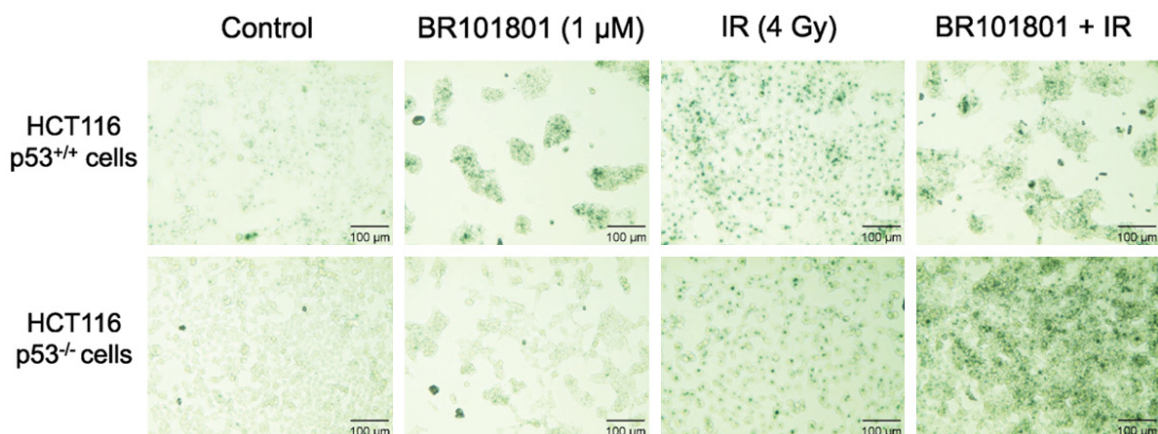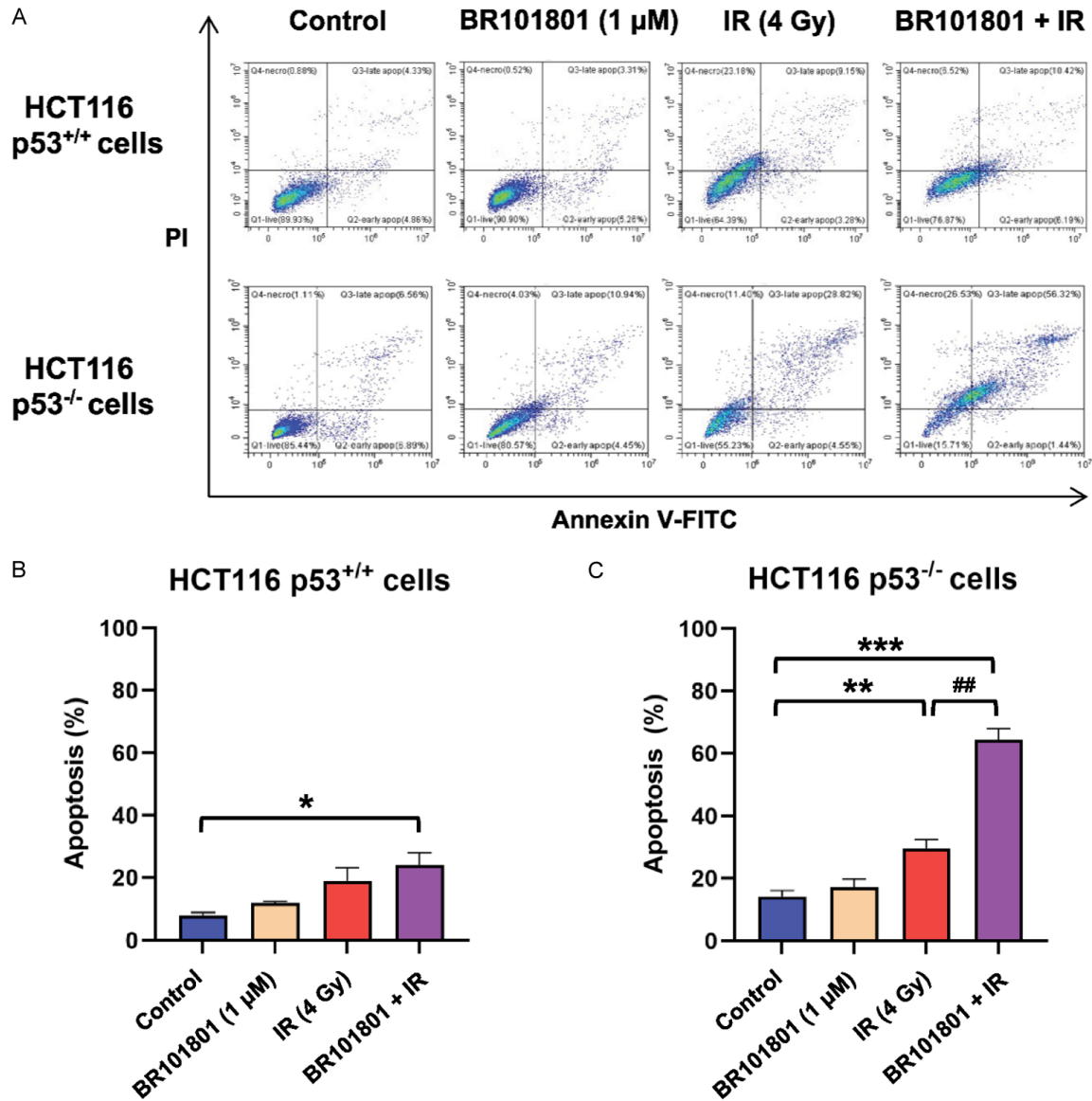

Figure 6. BR101801 accelerates IR-induced cellular senescence in HCT116 p53$^{-/-}$ cells. HCT116 p53$^{+/+}$ and HCT116 p53$^{-/-}$ cells were pretreated with 1 μM BR101801 for 24 h and irradiated with 4 Gy. After 24 h of IR, cells were stained with senescence-associated β-galactosidase staining solution to detect of senescence cells. Representative images were acquired using a light microscope. Scale bar = 100 μm (magnification, 20 ×). IR, ionizing radiation.

exhibited greater radiosensitivity than HCT116 p53$^{-/-}$ cells with an SF2 of 0.615. Interestingly, BR101801 could enhance the synergistic effects of radiotherapy in both the radiosensitive HCT116 p53$^{+/+}$ cells and relatively radioresistant HCT116 p53$^{-/-}$ human CRC cells. This enhancement was manifested as delayed DSB repair and the induction of apoptosis and cellular senescence in both radiosensitive and radioresistant HCT116 CRC cells, regardless of their p53 status *in vitro*. Notably, the augmented synergistic effects of BR101801 were more pronounced in HCT116 p53$^{-/-}$ cells than in HCT116 p53$^{+/+}$ cells. It has been reported that combining radiation therapy with DNA-PK inhibitors, such as M3814 and NU7441, can syner-

Figure 7. BR101801 promotes IR-induced apoptosis in the HCT116 p53$^{-/-}$ cells. HCT116 p53$^{+/+}$ and HCT116 p53$^{-/-}$ cells were pretreated with 1 µM BR101801 for 24 h and irradiated with 4 Gy. After 72 h of IR, apoptotic cells were stained with Annexin V and propidium iodide to stain the nuclei. (A) Flow cytometry analysis was performed to detect of apoptotic cells. Q1: live cells, Q2: early apoptotic cells, Q3: late apoptotic cells, Q4: necrosis cells. Quantitative analysis of apoptotic cells was included both early and late apoptotic cells of (B) HCT116 p53$^{+/+}$ cells and (C) HCT116 p53$^{-/-}$ cells. All data values are presented as the mean of three independent experiments ± standard error of the mean (SEM) ($^*P < 0.05$, $^{**}P < 0.05$ and $^{***}P < 0.001$ compared with control, $^{\#\#}P < 0.01$ compared with IR alone). IR, ionizing radiation.

gistically induce various modes of cell death, including apoptosis and senescence, in a p53-dependent manner [11, 12, 22]. Herein, the combined effect of BR101801 and radiation could induce robust apoptosis and senescence, even in p53-deficient cells, suggesting that the cell death pathways induced by combining BR101801 and radiation occur independent of the p53 status. The p53-p21 pathway is

an important signaling pathway in p53-dependent senescence, whereas the p16-p21 pathway plays a crucial signaling role in p53-independent senescence [23-25]. Moreover, a close relationship reportedly exists between telomere dysfunction and p53-independent apoptosis [26, 27]. It is plausible that BR101801 enhances the efficacy of radiation therapy by amplifying the radiosensitivity of
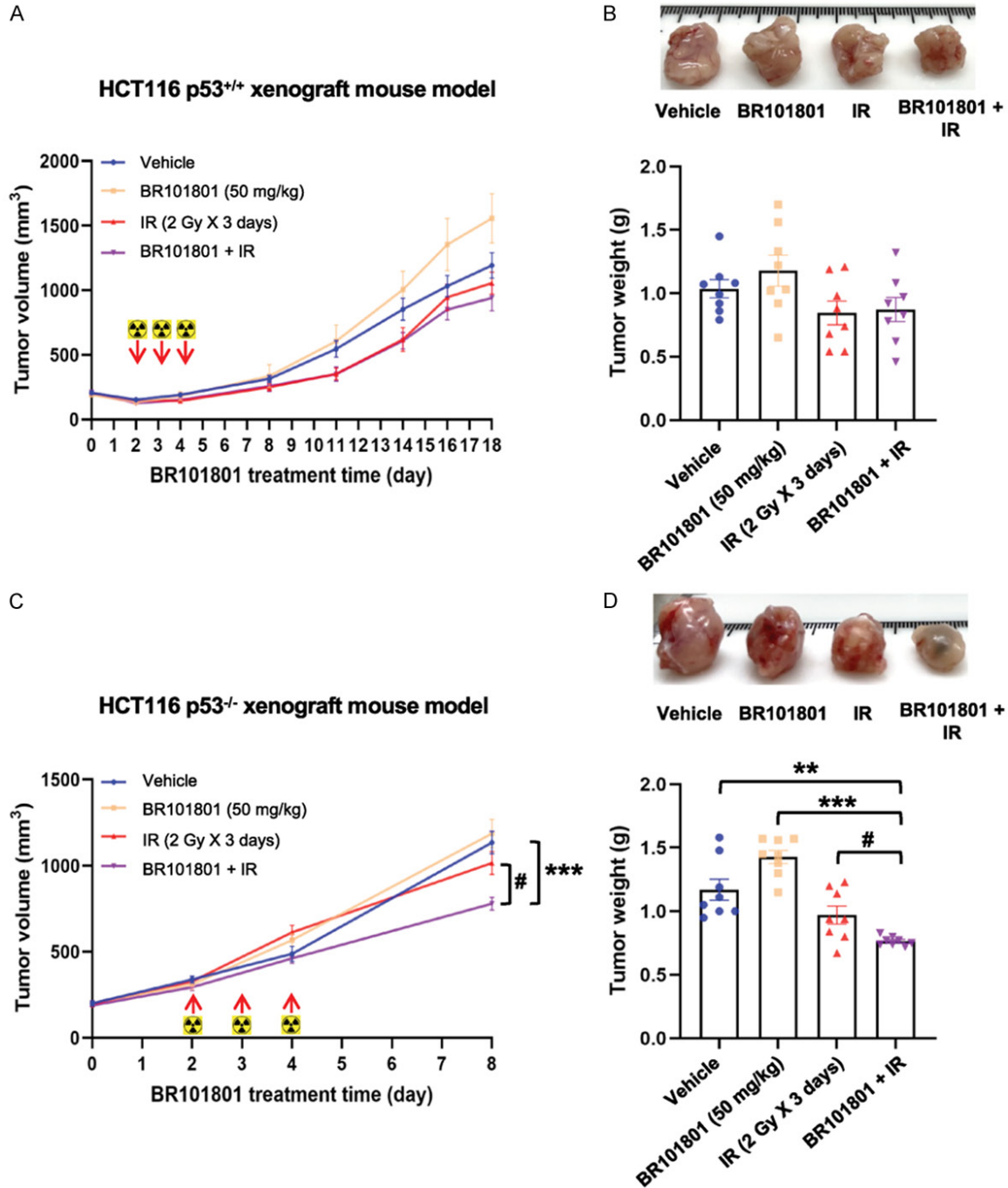
Figure 8. Combined treatment with BR101801 and IR exerts a radiosensitizing antitumor effect in the HCT116 p53$^{-/-}$ xenograft mouse model. Mice were divided into four groups: vehicle (n = 8), BR101801 (50 mg/kg, qd, n = 8), IR (2 Gy/day, for 3 days, n = 8), BR101801 + IR (n = 8). Mice were orally administered vehicle or BR101801 once daily when the tumor volume reached ~200 mm³. After two days of treatment, the tumor was locally irradiated with 2 Gy for three days. Tumor volume and tumor weight were compared between groups in (A), (B) HCT116 p53$^{+/+}$ xenograft mouse model and (C), (D) HCT116 p53$^{-/-}$ xenograft mouse model. All data values are presented as the mean of 8 mice per group ± standard error of the mean (SEM) ($^{**}P < 0.01$ and $^{***}P < 0.001$ compared with control or BR101801, $^{#}P < 0.05$ compared with IR alone). IR, ionizing radiation.

p53-deficient cancer cells via signaling pathways that operate independently of p53.

Despite observing synergistic effects on combining radiation with BR101801 in both HCT116

p53$^{+/+}$ and HCT116 p53$^{-/-}$ cells *in vitro*, the enhanced antitumor effects of combination treatment were solely evident in the xenograft models of HCT116 p53$^{-/-}$ cells. Conversely, the tumor growth rate in the vehicle-treated HCT116 p53$^{+/+}$ xenograft mouse model was slower than that in the HCT116 p53$^{-/-}$ xenograft mouse model. Notably, tumor growth inhibition lasted up to 7 days after the last irradiation, with tumor growth rebounding only 14 days later in the HCT116 p53$^{+/+}$ xenograft mouse model. This difference in the *in vivo* efficacy of combination treatment with BR101801 and IR might be attributed to the intricate influence of the tumor microenvironment. Moreover, loss of p53 function in tumor cells has been shown to increase hypoxia-inducible factor 1 (HIF-1) and vascular endothelial growth factor protein expression, resulting in enhanced angiogenesis and tumor growth upon hypoxia in HCT116 p53$^{-/-}$ xenograft mouse model [28]. Consistently, we detected angiogenesis in tumors of the vehicle, BR101801, and IR groups in the HCT116 p53$^{-/-}$ xenograft mouse model (Figure S1). Given that angiogenesis was not observed in the BR101801 + IR group, combination treatment with BR101801 and IR might have suppressed angiogenesis. DNA-PK is an upstream regulator of HIF-1 protein expression related to radioresistance in glioblastoma multiforme [29]. Accordingly, it can be postulated that BR101801 plays a role in overcoming resistance to radiotherapy by modulating the increased HIF-1 protein expression induced by loss of p53 function in the HCT116 p53$^{-/-}$ xenograft mouse model, which would elicit the mechanism underlying the antitumor efficacy of BR101801 in the p53-deficient xenograft mouse model.

In CRC, p53 dysfunction plays an important role in tumorigenesis and the development of resistance to radiotherapy by regulating various aspects of the tumor microenvironment, including hypoxia, blood vessels formation, cancer stem cells, and immune cell responses [5, 30-33]. The tumor microenvironment, which varies between genetic backgrounds and cell types, can substantially impact treatment outcomes. In this context, the presence of p53 deficiency can modulate the tumor microenvironment and thereby influence the response to treatment. The complexities of interactions between various components within the tumor microenvironment, like immune cells and tumor-associated factors, could potentially contribute to these observed differences. In-depth investigations are needed to gain a more comprehensive understanding of the effects of BR101801 on the tumor microenvironment associated with p53 deficiency in patients with CRC.

Although targeting the DDR pathway has been suggested as a novel therapeutic strategy for various solid cancers, its clinical application in CRC remains elusive and requires further preclinical investigation. BR101801, a new triple inhibitor of PI3K-γ/δ and DNA-PK, could suppress cellular proliferation and prolong DNA damage in HCT116 human CRC cells, regardless of their p53 status. Combined treatment with BR101801 and IR could substantially induce cell cycle arrest at the G2/M phase, apoptosis, and cellular senescence when compared with treatment with IR alone in HCT116 p53$^{-/-}$ cells. Based on preclinical data presented in the current study, the antitumor efficacy of combined BR101801 and radiotherapy may afford a new strategy for treating patients with radiotherapy-resistant CRC possessing p53 mutations or deficiencies. However, additional investigations and validation in clinical settings are indispensable to establish the clinical potential of this approach.

Disclosure of conflict of interest

None.

Address correspondence to: Dr. Youn Kyoung Jeong, Radiological and Medical Support Center, Korea Institute of Radiological and Medical Sciences, Seoul 01812, Republic of Korea. E-mail: amy3523@ kirams.re.kr; Dr. Byoung Soo Kim, Division of Applied RI, Korea Institute of Radiological and Medical Sciences, Seoul 01812, Republic of Korea. E-mail: bskim@kirams.re.kr

References

[1] Xi Y and Xu P. Global colorectal cancer burden in 2020 and projections to 2040. Transl Oncol 2021; 14: 101174.

[2] Siegel RL, Wagle NS, Cercek A, Smith RA and Jemal A. Colorectal cancer statistics, 2023. CA Cancer J Clin 2023; 73: 233-254.

[3] Hafner MF and Debus J. Radiotherapy for colorectal cancer: current standards and future perspectives. Visc Med 2016; 32: 172-177.

[4] Kong X, Yu D, Wang Z and Li S. Relationship between p53 status and the bioeffect of ionizing radiation. Oncol Lett 2021; 22: 661.

[5] Li XL, Zhou J, Chen ZR and Chng WJ. P53 mutations in colorectal cancer - molecular pathogenesis and pharmacological reactivation. World J Gastroenterol 2015; 21: 84-93.

[6] Gong L, Zhang Y, Liu C, Zhang M and Han S. Application of radiosensitizers in cancer radiotherapy. Int J Nanomedicine 2021; 16: 1083-1102.

[7] Brandsma I and Gent DC. Pathway choice in DNA double strand break repair: observations of a balancing act. Genome Integr 2012; 3: 9.

[8] Shrivastav M, De Haro LP and Nickoloff JA. Regulation of DNA double-strand break repair pathway choice. Cell Res 2008; 18: 134-147.

[9] Mladenov E, Magin S, Soni A and Iliakis G. DNA double-strand break repair as determinant of cellular radiosensitivity to killing and target in radiation therapy. Front Oncol 2013; 3: 113.

[10] Huang RX and Zhou PK. DNA damage response signaling pathways and targets for radiotherapy sensitization in cancer. Signal Transduct Target Ther 2020; 5: 60.

[11] Yu L, Shang ZF, Hsu FM, Zhang Z, Tumati V, Lin YF, Chen BP and Saha D. NSCLC cells demonstrate differential mode of cell death in response to the combined treatment of radiation and a DNA-PKcs inhibitor. Oncotarget 2015; 6: 3848-3860.

[12] Sun Q, Guo Y, Liu X, Czauderna F, Carr MI, Zenke FT, Blaukat A and Vassilev LT. Therapeutic implications of p53 status on cancer cell fate following exposure to ionizing radiation and the DNA-PK inhibitor M3814. Mol Cancer Res 2019; 17: 2457-2468.

[13] Fok JHL, Ramos-Montoya A, Vazquez-Chantada M, Wijnhoven PWG, Follia V, James N, Farrington PM, Karmokar A, Willis SE, Cairns J, Nikkila J, Beattie D, Lamont GM, Finlay MRV, Wilson J, Smith A, O'Connor LO, Ling S, Fawell SE, O'Connor MJ, Hollingsworth SJ, Dean E, Goldberg FW, Davies BR and Cadogan EB. AZD7648 is a potent and selective DNA-PK inhibitor that enhances radiation, chemotherapy and olaparib activity. Nat Commun 2019; 10: 5065.

[14] Lee JH, Jeon B, Park M, Ha J, Kim SJ, Son MK, Wang S, Lee JH and Jeong YK. Synergistic radiosensitizing effect of BR101801, a specific DNA-dependent protein kinase inhibitor, in various human solid cancer cells and xenografts. Am J Cancer Res 2021; 11: 5440-5451.

[15] Jeon B, Lee YJ, Shin J, Choi MJ, Lee CE, Son MK, Park JH, Kim BS, Kim HR, Jung KH, Cha JH and Hong SS. A combination of BR101801 and venetoclax enhances antitumor effect in DLBCL cells via c-Myc/Bcl-2/Mcl-1 triple targeting. Am J Cancer Res 2023; 13: 452-463.

[16] Fei P and El-Deiry WS. P53 and radiation responses. Oncogene 2003; 22: 5774-5783.

[17] Lee CL, Blum JM and Kirsch DG. Role of p53 in regulating tissue response to radiation by mechanisms independent of apoptosis. Transl Cancer Res 2013; 2: 412-421.

[18] Hernandez Borrero LJ and El-Deiry WS. Tumor suppressor p53: biology, signaling pathways, and therapeutic targeting. Biochim Biophys Acta Rev Cancer 2021; 1876: 188556.

[19] Jeong YK, Kim MS, Lee JY, Kim EH and Ha H. Metformin radiosensitizes p53-deficient colorectal cancer cells through induction of G2/M arrest and inhibition of DNA repair proteins. PLoS One 2015; 10: e0143596.

[20] Dahm-Daphi J. p53: biology and role for cellular radiosensitivity. Strahlenther Onkol 2000; 176: 278-285.

[21] Xu J, Patel NH, Saleh T, Cudjoe EK Jr, Alotaibi M, Wu Y, Lima S, Hawkridge AM and Gewirtz DA. Differential radiation sensitivity in p53 wild-type and p53-deficient tumor cells associated with senescence but not apoptosis or (nonprotective) autophagy. Radiat Res 2018; 190: 538-557.

[22] Sunada S, Kanai H, Lee Y, Yasuda T, Hirakawa H, Liu C, Fujimori A, Uesaka M and Okayasu R. Nontoxic concentration of DNA-PK inhibitor NU7441 radio-sensitizes lung tumor cells with little effect on double strand break repair. Cancer Sci 2016; 107: 1250-1255.

[23] Jacobs JJ and de Lange T. Significant role for p16INK4a in p53-independent telomere-directed senescence. Curr Biol 2004; 14: 2302-2308.

[24] Chan CH, Gao Y, Moten A and Lin HK. Novel ARF/p53-independent senescence pathways in cancer repression. J Mol Med (Berl) 2011; 89: 857-867.

[25] Rayess H, Wang MB and Srivatsan ES. Cellular senescence and tumor suppressor gene p16. Int J Cancer 2012; 130: 1715-1725.

[26] Afshar G, Jelluma N, Yang X, Basila D, Arvold ND, Karlsson A, Yount GL, Dansen TB, Koller E and Haas-Kogan DA. Radiation-induced caspase-8 mediates p53-independent apoptosis in glioma cells. Cancer Res 2006; 66: 4223-4232.

[27] Lechel A, Satyanarayana A, Ju Z, Plentz RR, Schaetzlein S, Rudolph C, Wilkens L, Wiemann SU, Saretzki G, Malek NP, Manns MP, Buer J and Rudolph KL. The cellular level of telomere dysfunction determines induction of senescence or apoptosis in vivo. EMBO Rep 2005; 6: 275-281.

[28] Ravi R, Mookerjee B, Bhujwalla ZM, Sutter CH, Artemov D, Zeng Q, Dillehay LE, Madan A, Semenza GL and Bedi A. Regulation of tumor angiogenesis by p53-induced degradation of hypoxia-inducible factor 1alpha. Genes Dev 2000; 14: 34-44.

[29] Marampon F, Gravina GL, Zani BM, Popov VM, Fratticci A, Cerasani M, Di Genova D, Mancini M, Ciccarelli C, Ficorella C, Di Cesare E and Festuccia C. Hypoxia sustains glioblastoma radioresistance through ERKs/DNA-PKcs/HIF-1alpha functional interplay. Int J Oncol 2014; 44: 2121-2131.

[30] Rivlin N, Brosh R, Oren M and Rotter V. Mutations in the p53 tumor suppressor gene: important milestones at the various steps of tumorigenesis. Genes Cancer 2011; 2: 466-474.

[31] Solomon H, Dinowitz N, Pateras IS, Cooks T, Shetzer Y, Molchadsky A, Charni M, Rabani S, Koifman G, Tarcic O, Porat Z, Kogan-Sakin I, Goldfinger N, Oren M, Harris CC, Gorgoulis VG and Rotter V. Mutant p53 gain of function underlies high expression levels of colorectal cancer stem cells markers. Oncogene 2018; 37: 1669-1684.

[32] Schulz A, Meyer F, Dubrovska A and Borgmann K. Cancer stem cells and radioresistance: DNA repair and beyond. Cancers (Basel) 2019; 11: 862.

[33] Pavlakis E and Stiewe T. p53's extended reach: the mutant p53 secretome. Biomolecules 2020; 10: 307.
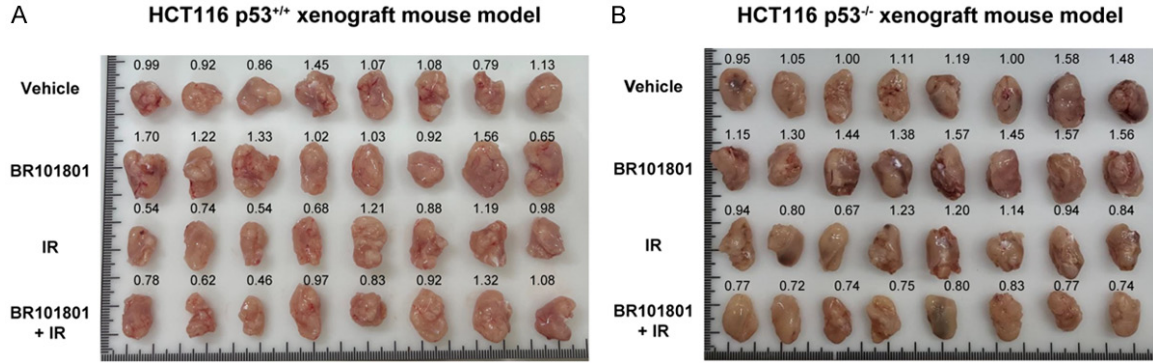
Figure S1. Combined treatment with BR101801 and IR inhibits tumor growth in the HCT116 p53$^{-/-}$ xenograft mouse model. When the tumor volume reached ~200 mm^3, mice were orally administered vehicle or BR101801 (50 mg/kg) once daily. After two days, the tumors of mice in the IR alone group and BR101801 + IR group were locally irradiated (2 Gy) for three days using a ^{60}Co gamma-ray irradiator. Images representing excised tumors from (A) HCT116 p53$^{+/+}$ xenograft mouse model and (B) HCT116 p53$^{-/-}$ xenograft mouse model, when the tumor volume of the vehicle group reached approximately 1000 mm^3. The tumor weight (g) corresponding to each tumor is indicated above the tumor.